Role of residual water hydrogen bonding in sugar/water/biomolecule systems: a possible explanation for *trehalose peculiarity*

2007 J. Phys.: Condens. Matter 19 205110

(http://iopscience.iop.org/0953-8984/19/20/205110)

IOP PUBLISHING JOURNAL OF PHYSICS: CONDENSED MATTER

J. Phys.: Condens. Matter **19** (2007) 205110 (16pp) doi:10.1088/0953-8984/19/20/205110

Role of residual water hydrogen bonding in sugar/water/biomolecule systems: a possible explanation for *trehalose peculiarity*

L Cordone, G Cottone and S Giuffrida

Dipartimento di Scienze Fisiche ed Astronomiche, Università di Palermo and CNISM, Italy

E-mail: cordone@fisica.unipa.it

Received 6 November 2006, in final form 3 January 2007
Published 25 April 2007
Online at stacks.iop.org/JPhysCM/19/205110

Abstract

We report on the set of experimental and simulative evidences which enabled us to suggest how biological structures embedded in a non-liquid water–saccharide *solvent* are anchored to the surrounding matrix via a hydrogen bond network. Such a network, whose rigidity increases by decreasing the sample water content, couples the degrees of freedom of the biostructure to those of the matrix and gives place to protein–saccharide–water structures (*protein–solvent conformational substates*). In particular, the whole set of data evidences that, while the protein–sugar interaction is well described in terms of a *water entrapment* hypothesis, the *water replacement* hypothesis better describes the sugar–membrane interaction; furthermore, it gives a hint towards the understanding of the origin of the *trehalose peculiarity* since the biomolecule–matrix coupling, specific to each particular sugar, always results in being the tightest for trehalose.

In line with the heterogeneous dynamics in supercooled fluids and in carbohydrate glasses of different residual water contents, recent results confirm, at the single molecule level, the existence of *protein–solvent conformational substates*, spatially heterogeneous and interconverting, whose rigidity increases by lowering the sample hydration.

1. Introduction

Trehalose, a disaccharide composed of two (1 → 1)-linked alpha, alpha units of glucopyranose (figure 1), is a non-reducing disaccharide of glucose found in large quantities in organisms that can survive adverse environmental conditions such as extreme drought and high temperatures [1–4] under a condition, known as *anhydrobiosis*, in which all metabolic processes are blocked. These organisms can be kept dry and apparently dead for several years, and upon rehydration, their vegetative cycle restarts. This process can be repeated several

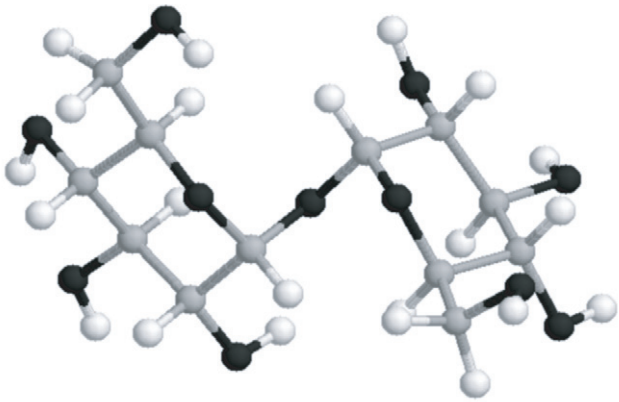

Figure 1. Trehalose molecule. Black spheres: oxygen atoms; dark grey: carbon atoms; light grey: hydrogen atoms.

times with no apparent damage to the organisms. It has been reported that the stabilizing role against the adverse conditions is played by trehalose [5, 6]. Furthermore, it has been observed that isolated structures, such as enzymes or liposomes, are preserved against stressing conditions when embedded in trehalose matrices [7, 8]. An analogous protective effect is also accomplished by other saccharides, although trehalose is the most effective in terms of structural and functional recovery [7]. Several studies have been performed on sugar–water–biomolecule systems by experimental [9–29] and simulative techniques [30–37]. The main hypotheses proposed for the trehalose–biomolecule interaction are:

(i) the *water replacement hypothesis*, according to which stabilization occurs via the formation of hydrogen bonds between the sugar and the biostructure; indeed, trehalose binds to protein carboxyl groups, as evidenced by the appearance of the carboxylate band at 1580 cm^{-1} in freeze-dried mixtures [38] or by the influence of proteins on the infrared spectra of dried carbohydrates [9];
(ii) the water-entrapment hypothesis, according to which, in the dry state, trehalose rather than directly binding to proteins traps the residual water at the biomolecule sugar interface by glass formation (*preferential hydration hypothesis*) [10];
(iii) the high viscosity hypothesis, according to which viscosity effects cause motional inhibition [39] and hindering of processes leading to loss of structure and denaturation. In this respect, Green and Angell [40] suggested the rather high glass transition temperature of trehalose with respect to other glass forming sugars to be responsible for the trehalose peculiarity.

The above hypotheses are not mutually exclusive. The formation of a glassy state does not imply hydrogen bonding, as evidenced by measurements on dextran [38]. The effectiveness of trehalose in preservation may be due to the ability of forming glassy structures in a wide hydration range, along with the hydrogen bond capability. However, this is not consistent with results on raffinose, which is less effective than other sugars [41], although it has a glass transition temperature comparable with that of trehalose, together with larger hydrogen bonding potential [42, 43].

A large part of the simulative and experimental work aimed at understanding, at the molecular level, the origin of the *trehalose peculiarity* has been performed on binary water–sugar systems, in wide ranges of sugar concentration and temperature, by exploiting several

experimental and computational procedures. Results concurred in indicating that the presence of trehalose sizably modifies the hydrogen bond network and the water dynamics; in particular, a large destructuring effect on the water tetrahedral hydrogen bond network has often been invoked to explain the effectiveness of trehalose as a bioprotectant, since it prevents the low-temperature water crystallization (see [44] and references therein). It has been suggested that by binding water molecules more tightly, the glass formed by trehalose could reduce molecular motion leading to its bioprotective effects [44, 45]. In particular, a comparison with sucrose pointed out that, due to the formation of internal hydrogen bonds, sucrose results in being more rigid and less hydrated than trehalose, since the internal bonds leave a lower number of sites available for interactions with water [46]; maltose, notwithstanding the similarity in hydration number, restrains the surrounding water molecules less than trehalose [47]. Furthermore, maltose–water solutions, in contrast to other saccharide–water systems, resulted in inhomogeneous systems, in which maltose molecules cluster [48]. Such clustering was suggested to likely be due to the dipole moment of this disaccharide, which is much larger than for the other saccharides [49].

In general, the studies devoted to understanding the origin of the trehalose peculiarity tried to find a *single* biomolecule–sugar mechanism of interaction, working both for proteins and membranes. In contrast (see below), molecular dynamics (MD) simulations and experimental results suggest that while *preferential hydration* seems to be the dominant mechanism in the interaction between globular proteins and sugar [31–33, 49], *water replacement* by saccharides occurs in membrane–sugar–water systems [8, 34–37].

2. Dynamics and structural behaviour of biomolecules embedded in water–saccharide solvent

2.1. Proteins

Several experimental studies have been performed on sugar–water biomolecule systems [11–29] aimed at ascertaining the effects of the sugar matrix on the dynamics of the embedded biomolecule and the eventual coupling between the biostructure and the external matrix. Such studies included flash photolysis on carboxy-myoglobin (MbCO) [11–15, 19], Mössbauer spectroscopy [25, 16], incoherent elastic neutron scattering [26, 29], kinetic hole burning [18, 20], infrared vibrational echo [17, 23, 24], and functional behaviour of the reaction centre of *Rhodobacter Sphaeroides* [50–53]. All the above experiments pointed out how embedding proteins in saccharide matrices of low water content sizably reduces the internal protein dynamics; furthermore, it was shown that the content of residual water modulates the dynamics and structural evolution of the protein and of the external matrix [54]. Such information evidenced how embedding protein in water–sugar systems, in which the amount of residual water is varied, could be a useful tool for investigating the temperature dependence of the protein dynamic structure function relationship at different solvent rigidity, thus enabling one to disentangle the rigidity from temperature effects.

2.1.1. Molecular dynamics (MD) simulations. The sizable reduction of the internal protein dynamics was also evidenced in an MD simulation of an MbCO molecule embedded in a plasticized amorphous trehalose matrix 89% trehalose/[trehalose + water] w/w [30, 31, 33]. Furthermore, MD simulations also showed that, in trehalose–water–protein systems, structures are formed in which trehalose molecules are mainly bound to the protein through single hydrogen bonds, and water molecules are in excess over their concentration in the bulk solvent [31]. In such structures, a hydrogen bond (HB) network connects groups at the

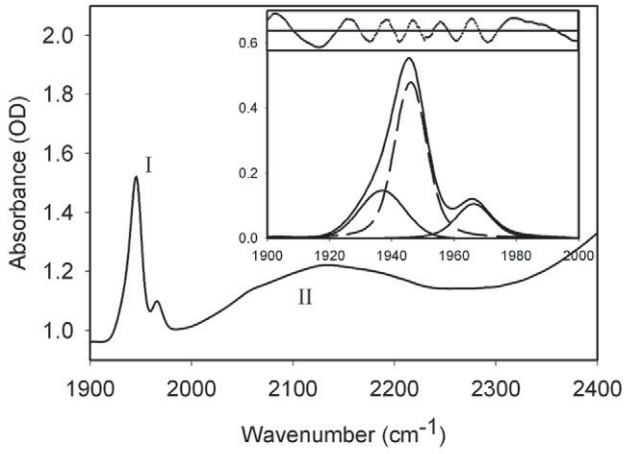

Figure 2. CO stretching band (I, 1900–2000 cm^{-1}) and association band of water (II, 2000–2400 cm^{-1}) in trehalose-coated MbCO. The inset shows the fitting of the CO band in terms of three taxonomic A substates [61]. Data refer to a humid sample, at $T = 300$ K. Figure taken from [55].

myoglobin surface, water molecules and trehalose molecules. In this network, the fraction of water molecules forming multiple hydrogen bonds with both protein and sugar increases when the water content is decreased. Considering that the water motional freedom decreases by increasing the number of hydrogen bonds in which each molecule is involved, one has that the water dipole network must exhibit a decrease of the thermal rearrangements by reducing the residual water [55–57, 49]. Furthermore, according to the suggestion that the structural relaxation of a protein is coupled to the relaxation of the hydrogen bond network [58–60] the above decreased rearrangements will be reflected, as experimentally observed, in a decrease of the protein thermally induced structural variations, when the water content is decreased.

Results from MD simulations in which one MbCO molecule was embedded in sucrose–water [33] or maltose–water (work in preparation) at the same concentration as in trehalose [89% w/w] [30, 31], point out that some regions of the protein chain exhibit a larger flexibility in sucrose and maltose than in trehalose. Furthermore, the increase of the water mean square displacement with time is the lowest in maltose, in full agreement with the results on maltose–water systems, in which maltose molecules cluster and water might remain trapped at these clusters [48, 49].

2.1.2. Fourier transform infrared (FTIR) measurements. As mentioned, several experiments showed that embedding protein in water–sugar matrices of low water content sizably reduces the dynamics of the embedded protein; however, the measurements that evidenced such a reduction [11–29] did not give any hints towards the understanding of the mechanisms at the basis of the observed effect. Experimental information on such mechanisms was obtained by simultaneously following the temperature dependence (300–20 K) of the bound CO and of the water association band in samples of MbCO embedded in sugar matrices of low water content [49, 55–57].

The stretching band of the bound CO in MbCO (see figure 2) is split into three different sub-bands, which correspond to three specific different environments experienced by the bound CO within the heme pocket [61, 62]. These sub-bands reflect the populations of the three

taxonomic A and lower tier conformational substates, and depend on external parameters such as pH, temperature, and pressure [63–67]. Accordingly, the thermal behaviour of such sub-bands conveys information on the heme pocket structural variations, which affect the whole shape of the CO stretching band. As shown in figure 2, on the high-frequency side of the CO stretching band there appears the water association band, which is attributed [68] to a combination of the bending mode of water molecules with intermolecular vibrational modes. Furthermore, the coupling of the bending modes of water molecules with intermolecular vibrational modes involving non-water OH groups (arising e.g. from sugar or protein H bond forming groups) also contributes to the band [55].

The coupling between heme pocket and external matrix in *trehalose-coated* MbCO was evidenced by FTIR measurements, in which the thermal behaviour of the CO stretching and of the water association bands was analysed in the temperature range 263–323 K [28]. The study was afterwards extended to a larger temperature interval (300–20 K) in which three MbCO–trehalose–water samples of low water content were studied [55–57, 49]. Figures 3 and 4 respectively show, superimposed, the stretching band of the bound CO and the water association band for the above three samples, in the temperature interval 300–20 K. The thermal evolution of both the CO stretching and water association bands was put on a quantitative ground by plotting the spectral distance (SD) of the various normalized spectra from the respective normalized spectrum measured at 20 K. This is defined as [55]

$$\mathrm{SD} = \left\{ \int_{\nu} [A(\nu, T) - A(\nu, T = 20\ \mathrm{K})]^2 \, \mathrm{d}\nu \right\}^{1/2} \approx \left\{ \sum_{\nu} [A(\nu, T) - A(\nu, T = 20\ \mathrm{K})]^2 \Delta\nu \right\}^{1/2} \tag{1}$$

where $A(\nu)$ is the normalized absorbance at frequency ν and $\Delta\nu$ is the frequency resolution. The above quantity represents the deviation of the normalized spectrum at temperature T from the normalized spectrum at 20 K; for the protein it reflects the overall thermally induced heme pocket structural changes evidenced by the changes in the population of taxonomic (A) and lower hierarchy substates. Furthermore, in view of the structured profile of the water association band, it was assumed that, for this band, the SD reflects thermally induced structural rearrangements of the water molecule network within either the solid or plasticized amorphous samples [55–57, 49].

Figure 5 shows the spectral distances (see equation (1)) of the CO stretching and of the water association bands (respectively, $\mathrm{SD_{CO}}$ and $\mathrm{SD_{WATER}}$). The figure evidences the small temperature dependence of both the CO and the water band in the very dry sample, as compared to the other two samples. In particular, in contrast to the driest sample, the last two are already temperature dependent at ∼50 K; moreover, their SDs are almost coincident up to ∼180 K, while above such temperature the most water-rich sample exhibits larger increase. As mentioned above, SDs relative to the CO stretching band convey condensed information on the thermal evolution of the heme pocket structure as experienced by the bound CO, while SDs relative to the water band convey condensed information on the thermal evolution of the matrix structure, as experienced by the water molecules. The data in figure 5 evidence the strict structural coupling between the internal degrees of freedom of the heme pocket to those of the external matrix. The structural fluctuations involving displacement of the protein surface are severely hindered when the protein is embedded in a solid trehalose glass [17]. Accordingly, the data in figure 5 were interpreted by considering that the two drier samples are, in the whole temperature range investigated, solid glasses in which the temperature dependence of $\mathrm{SD_{CO}}$ arises from protein atom motions with respect to the centre of mass (*internal* processes), which take place without displacement of the protein surface and involve low hierarchy substates. In contrast, the humid sample behaves as a solid glass

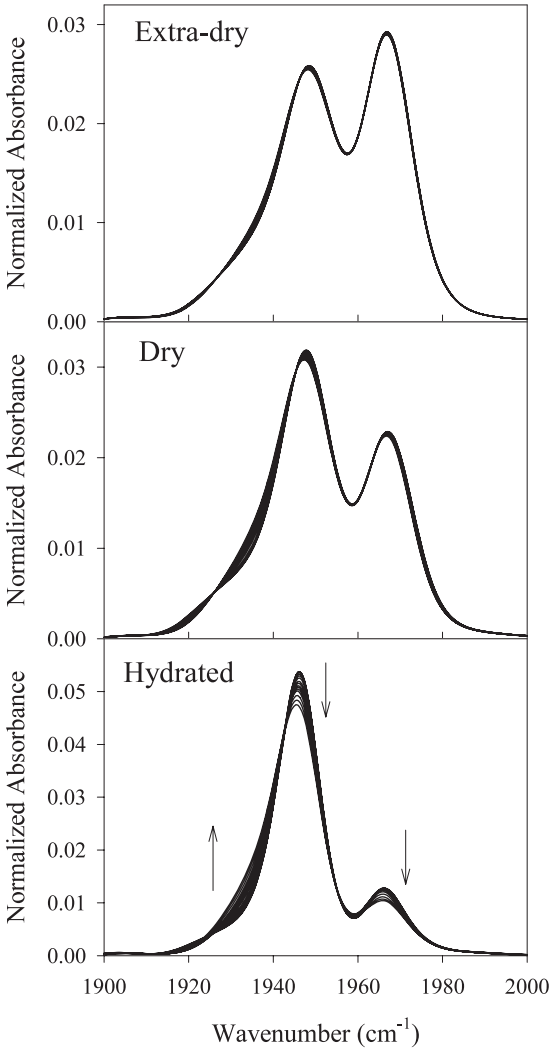

Figure 3. Normalized spectra of the CO stretching band in the range 300–20 K. Upper panel: very dry sample; central panel: dry sample; lower panel: humid sample; the water/trehalose molar ratio respectively was ∼0.3, ∼2 and ∼30. Samples were prepared by initially drying, at room temperature, aliquots of an aqueous trehalose–MbCO solution, layered on CaF_2 windows of ∼1 cm^2 surface, in a desiccator under a CO atmosphere. The very dry sample was prepared by further drying within the cryostat by heating, under vacuum at 353 K, until exhaustive dehydration, before starting measurements. The dry sample was dried under vacuum at 353 K, and then shortly exposed to room moisture. The humid sample was equilibrated with 60% humidity at 300 K before measurements. For details, see [55].

only in the temperature interval 20–180 K. At temperatures higher than ∼180 K the sample becomes a plasticized amorphous system in which structural rearrangements of the protein are accompanied by surface displacement [17, 54]. This behaviour, in particular, indicated that the low-frequency motions of the heme environment, which take place in liquid solutions [69], could be populated only in the humid sample and only at the highest temperature. Therefore, coupling of the CO vibration with large-amplitude, low-frequency motions is not expected to sizably alter the shape of the CO stretching band in our sample.

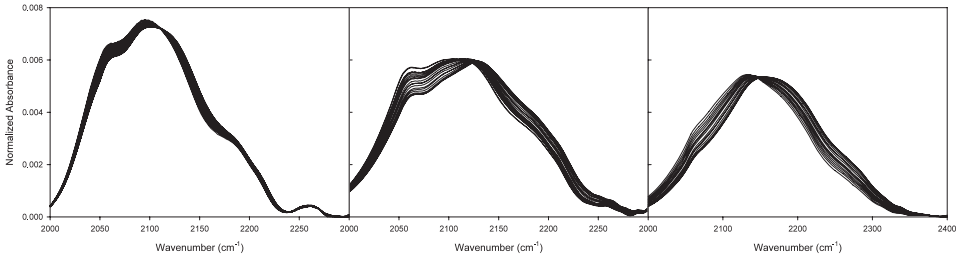

Figure 4. Normalized spectra of the water association band in the range 300–20 K. Left panel: very dry sample; central panel: dry sample; right panel: humid sample.

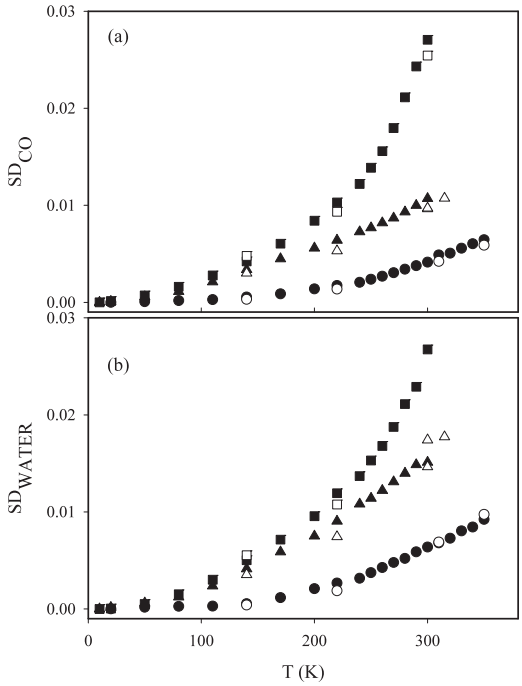

Figure 5. (a) CO stretching band spectra distance (SD_{CO}) referred to the spectrum measured at 20 K versus temperature; (b) water association band spectra distance (SD_{WATER}) referred to the spectrum measured at 20 K versus temperature. Circles: very dry sample; triangles: dry sample; squares: humid sample. Full symbols: data points obtained during cooling; open symbols: data points obtained during heating. The very good reproducibility of the data points indicates that the systems are in thermal equilibrium. Figure taken from [55].

To get closer information on the correlation between the thermal evolution of the protein and of the external matrix structure (see figure 6), SD_{CO} was plotted as a function of SD_{WATER}. As is evident, the evolution of the structure of the protein and of the matrix exhibits a single linear correlation, almost independent of water content, for the two drier samples in the whole temperature range investigated. In contrast, a deviation, which becomes sizable at ∼180 K, is evident for the humid sample. It is conceivable that at this temperature the water HB network collapses and translational displacement of protein-bound water takes place; this in turn [58–60] enables large-scale substate interconversion and protein structural relaxations. These motions, which involve displacements of the protein surfaces [54–57, 49], have been

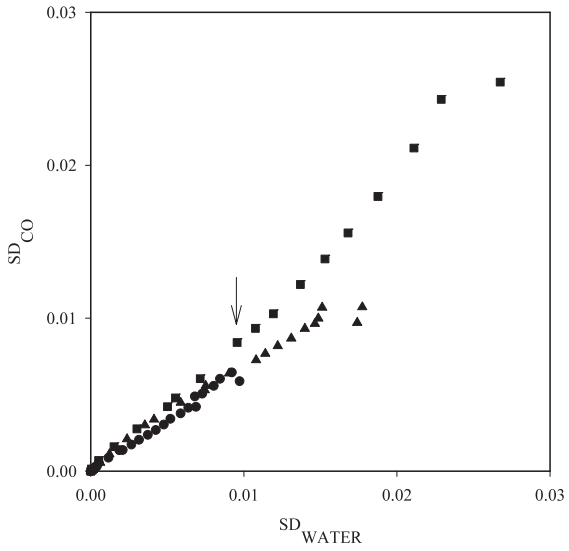

Figure 6. Plot of SD_{CO} versus SD_{WATER}. Circles: very dry sample; triangles: dry sample; squares: humid sample. The arrow indicates the point corresponding to $T \sim 180$ K for dry and humid samples. Figure taken from [55].

suggested to be driven by fluctuations of the dielectric constant of the medium [70], which, indeed, imply water molecule translational freedom.

In order to obtain insights on the origin of the trehalose peculiarity, analogous FTIR measurements were performed on samples in which MbCO was embedded in matrices of different sugars (glucose, maltose, sucrose, raffinose) and content of residual water [49]. The analysis of the thermal behaviour of the spectra distance relative to both the stretching band of the ligand CO molecule (SD_{CO}) and the water association band (SD_{WATER}) showed that the thermal evolution of sugar–water matrix barely depends on the particular saccharide, while the protein internal motions resulted in being regulated in a way which is specific to each sugar. A plot of SD_{CO} versus SD_{WATER} showed that the slope of the correlation curve was the lowest for trehalose, thus indicating a tighter coupling in this sugar. This result gave a hint towards the understanding of the origin of best efficiency of trehalose with respect to the other studied saccharides as a bioprotectant; indeed, the appearance of damages on biological structures will involve more structural variations of the surrounding matrix in trehalose than in other saccharides.

2.1.3. Flash photolysis experiments on MbCO embedded in trehalose–water matrices. The FTIR data reported open the question of how the constraints, imposed on the protein by the external matrix, affect the functional properties such as for example the CO rebinding after flash photolysis [11–15, 19, 54] or the electron transfer process in photosynthetic reaction centres [50–53]. The rebinding of ligands to Mb following laser photolysis has been extensively used to understand the molecular mechanisms underlying protein–ligand interactions [71–81]; indeed, such rebinding occurs through a complex pathway resulting from protein relaxation and movements of the ligand within the protein [79–81].

Information on such complex pathways has been obtained by studying the rebinding of the photodissociated CO molecule in MbCO embedded in saccharide matrices of different but low water content [54]. Indeed, as mentioned, this procedure enables one to disentangle temperature

from rigidity effects [49] enabling one to alter the dynamics of the protein and of the external matrix, leaving the thermal energy of the photodissociated CO unaltered.

In line with FTIR data, decreasing the sample water content sizably accelerates the rate of the CO rebinding, in full agreement with the existence of an HB network, which anchors the protein surface to the surrounding solid matrix, thus hindering substrate interconversion and protein relaxation [11, 54, 82].

Room-temperature experiments were also performed in MbCO–trehalose samples, briefly illuminated prior to the laser pulse [82]. Pre-illumination was found to decrease the rate of CO rebinding with respect to non-pre-illuminated samples in dry but not in humid samples. This was thought to arise from the continuous attempts performed by the protein, during pre-illumination, to undergo relaxation towards the photodissociated deoxy state; this causes the collapse of the rigid HB network, thus causing a decoupling of the internal degrees of freedom of the protein from those of the external matrix. Lack of conformational relaxation following photoexcitation and protein–matrix decoupling, following continuous illumination, were also observed in the reaction centre of *Rhodobacter sphaeroides* [50–52].

2.2. Membranes

It is well established that disaccharides stabilize biological membranes [7]. In particular, studies on liposome embedded in sugar matrices have shown that the addition of sugar lowers the melting temperature of bilayer membranes [1], thereby preventing leakage and fusion during drying and freeze-drying [7].

2.2.1. Molecular dynamics simulations. Results from molecular dynamics simulations showed that the interaction of trehalose molecules and lipids occurs at the surface of the bilayer [34, 35, 37]. The sugar molecules adopt specific conformation to fit onto the surface of the bilayer, interacting with more than one lipid simultaneously; by bridging adjacent lipids, trehalose molecules prevent them from aggregating or collapsing [34]. In contrast, results from other simulations [36] pointed out how trehalose tends to be oriented parallel to the membrane normal, making multiple hydrogen bonds with the lipids and penetrating deeper in the membrane. In any event, results from simulative studies concur in supporting, in contrast to proteins, a direct interaction of trehalose with membranes, according to the *water replacement* hypothesis, formulated on the basis of several experimental measurements, including infrared spectroscopy, nuclear magnetic resonance and x-ray diffraction (see [8] and references therein).

2.2.2. FTIR measurements. Recently, FTIR measurements have been performed on cholate-containing liposomes (CCLs) embedded in trehalose or sucrose matrices with different residual water content [8]. Information on the CCL phase transition was obtained by following the thermal evolution (310–70 K) of the IR spectrum of the carbonyl moieties of phospholipids, in the frequency range 4225–4550 cm^{-1}, shown in figure 7.

It is well known that lipid phase transition implies rearrangements at supermolecular level, and is reflected in sudden correlated changes of several parameters such as for example peak frequency or line-width [83]. Accordingly, the phospholipid phase transition was followed [8] through the thermal evolution of the spectral distance (SD) of the CH_2 normalized spectra referred to the respective lowest-temperature normalized spectrum. Figure 8 shows the temperature dependence of SD_{CH_2} relative to a dry and a wet trehalose sample. The continuous line represents the fitting in terms of the sum of a sigmoid and a straight line [8]. The plot in the figure evidences the lipid phase transition from gel to liquid crystal phase. The same behaviour

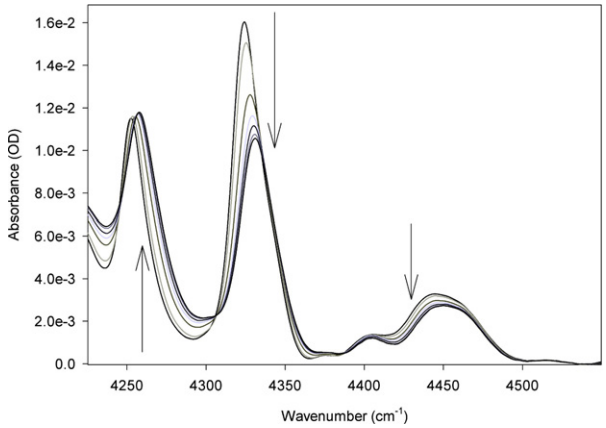

Figure 7. Methylenic absorption bands in the temperature interval 310–75 K for a dry trehalose sample. Data are plotted after subtraction of a broad Gaussian extrapolation. Figure taken from [8].

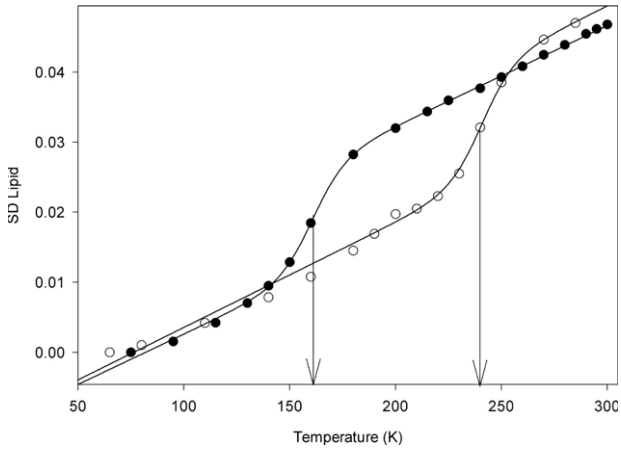

Figure 8. Spectral distance computed in the spectral zone 4225–4550 cm^{-1} for the dry T sample (●); wet T sample (○). The arrows indicate the midpoints of the sigmoid. Figure taken from [8]. For details of sample preparation, see [8].

is observed if the peak frequencies of the CH_2 combination band as a function of temperature are plotted instead of the spectral distance (data not shown; see [8]).

Figure 9 shows the water association band measured respectively in a dry and in a wet sample of trehalose-coated CCL at 300 K, together with the fittings performed in terms of five Gaussian, one Lorentzian and one Voigtian extrapolation.

To verify the eventual coupling of the lipid structure to the surrounding water–saccharide matrix, the thermal evolution of the peak frequency of the various sub-bands in figure 9 was analysed. Such analysis showed a very tight coupling between the small sub-band at ∼2025 cm^{-1} and the alkyl chain structure. Indeed, the sub-band, which is absent in cholate-free liposomes, exhibits a sudden variation, in concurrence with the lipid phase transition, as evidenced in figure 10, which shows a plot of T_m plotted against T_{2025}, i.e., the midpoint of the sigmoid that represent the thermal evolution of the sub-band at 2025 cm^{-1} of the

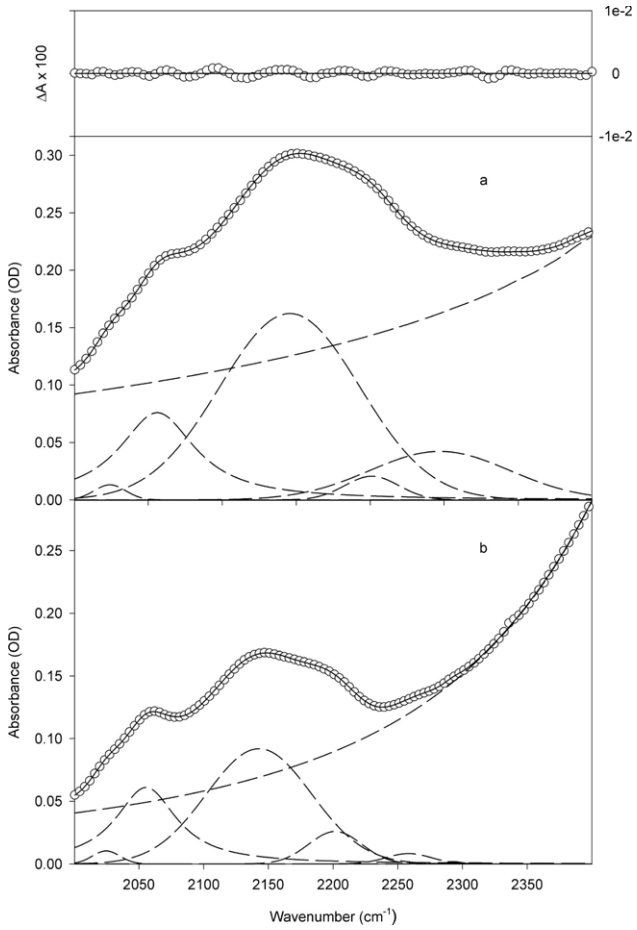

Figure 9. Water association band in wet T (panel (a)) and dry T (panel (b)) samples, at 300 K. The continuous curve represents the Gaussian extrapolation; the open circles represent the data. The other curves are the result of absorption profile decomposition. In the upper part of the graph, residues in expanded scale are represented, relative to the fitting shown in panel (a); similar residues are also obtained for the fitting in panel (b). Figure taken from [8].

water association band. It is noteworthy that such a small band must be ascribed to the presence of water molecules since, like the whole water association band, it is absent in dry samples of phosphatidylcholine and/or cholic acid. In particular, it was attributed to water molecules inserted within the lipidic structure in the neighbourhood of cholic acid in the region located at the border between the hydrophilic and the hydrophobic moieties of phospholipids. These water molecules, acting as lubricant at the contacts between the lipid polar heads, were suggested to be responsible for the peculiar flexibility of cholate-containing liposomes [84]. Furthermore, since different phospholipid headgroups structure corresponds to different lipid phases, the lipid phase transition is also reflected in a reorganization of water molecules in the surrounding of the CCL, as observed.

Figure 11 shows the temperature dependence of the spectral distance of the whole water association band (SD_{WATER}) for the same trehalose samples of figure 8. The data in figure 11 show a much looser coupling to the lipid phase transition than the small water sub-band at

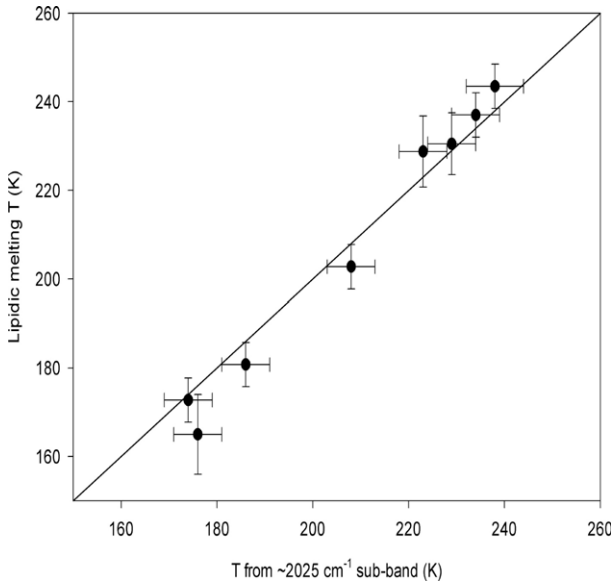

Figure 10. Lipidic melting temperature (T_m) plotted against the midpoint of the sigmoid which represent the thermal evolution of the sub-band at ∼2025 cm^{-1} of the water association band (T_{2025}). The continuous line is a straight line of unitary slope. Figure taken from [8].

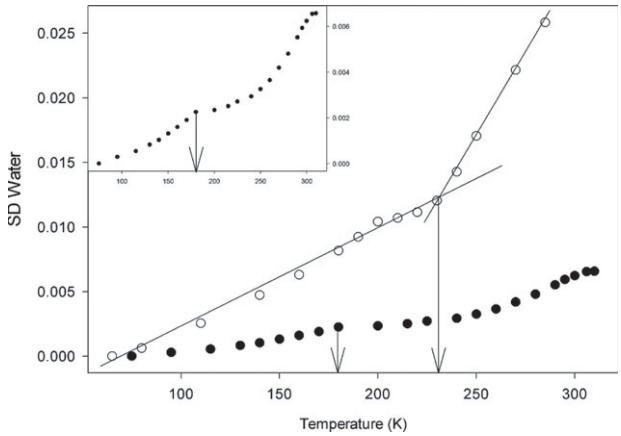

Figure 11. Spectral distance computed for the water association band spectral zone for dry T(●) and wet T(○) samples. The inset shows dry sample data in an expanded scale. The arrows indicate a discontinuity in the first derivative of the plotted curves. Figure taken from [8].

2025 cm^{-1}. Indeed, only a slope change of SD_{WATER} is observed, corresponding to the lipidic transition temperature. This was thought to stem from a loose coupling between the lipid phase transition and the external matrix. A loose coupling was, indeed, expected based on the *water replacement* hypothesis holding for sugar–membranes [9, 34–37], according to which water molecules in the surrounding matrix must be less directly involved than in the case of proteins.

Indeed, in water–trehalose–protein systems, the interactions between the macromolecule and the sugar are restricted to sites which bind mobile, singly hydrogen-bonded water molecules [85], and water molecules concentrate in the surroundings. In contrast, in the sugar–

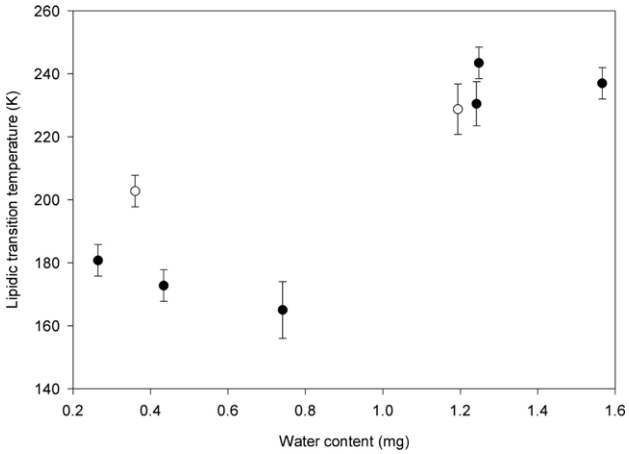

Figure 12. Lipid phase transition temperature as a function of sample water content. Open circles (○) sucrose; closed circles (●) trehalose. The error bars shown represent the maximum T_m difference among the estimates in the different spectral regions. Figure taken from [8].

liposome–water systems, the sugar is tightly bound to polar headgroups at the hydrophilic liposome interface, and a fraction of the liposomes hydrogen bonds forming sites bind water molecules. In this respect Crowe [86] reported a slope break, corresponding to the lipid phase transition, in a plot of trehalose OH stretching versus temperature, indicative of a coupling between the lipid phase transition and the surrounding medium, in trehalose-coated liposomes.

Figure 12 shows the transition temperature values (T_m) as a function of the samples' water content, both for trehalose and sucrose samples; the data points represent the average of the values obtained from the peaks at ∼4250, 4325 and 4340 cm^{-1}. As is evident from the figure, the transition temperature increases with increasing water content of the sample. As already mentioned, in samples of *trehalose-coated* proteins, structural rearrangements of the embedded protein sizeably decrease by the drying of the sample. This result could appear to be in contrast with the T_m decrease observed by the drying of trehalose- or sucrose-coated CCL. Such a T_m decrease, well known and established [1], has been rationalized by considering that, upon dehydration, trehalose prevents the close approach of headgroups. This makes the relative distance among the lipid moieties increase, causing a decrease in van der Waals interactions, which eventually leads to the observed lowering of the phase transition temperature. Furthermore, while wet samples show similar T_m either in sucrose or in trehalose, a difference appears in dry samples. This difference is consistent with data on carboxy-myoglobin embedded in trehalose or sucrose matrices, which show that the protein is more *tightly bound* in the former than in the latter system, particularly in dry systems [56, 33].

A point emerging from an inspection of the data in figure 12 is the apparent sigmoidal behaviour of the phase transition temperature in trehalose-coated CCL as a function of sample water content; such behaviour is indicative of a cooperative transition among liposome–sugar–water structures of different water content, stemming from cooperative collapse–reformation of hydrogen bond networks in the structures.

3. Spatial heterogeneity of the protein–solvent coupling

In MbCO embedded in trehalose–water matrices the thermal interconversion among taxonomic A substates is progressively hindered, when residual water decreases from very humid to

very dry samples [28, 54, 55]. Since the distribution of conformational substates at a given temperature is an equilibrium property, the observed progressive reduction of interconversion in non-solid matrices (during sample dehydration) suggested that such a process should not be related to the increasing viscosity. Alternatively, considering that the dynamics in glass-forming systems is spatially heterogeneous [87, 88], one can conceive that, during the drying, the sample behaves as a heterogeneous system in which only a fraction of proteins molecules is allowed to fluctuate among different conformational substates. In contrast, for the remaining fraction (which increases by decreasing the water content), the fluctuations driving the crossing of the energy barriers are hindered. Based on this assumption, the progressive inhibition of interconversion during the drying was suggested to arise from a spatially heterogeneous protein–solvent coupling due to the simultaneous presence of *'interconverting'* protein–water–sugar structures of different hardness (*protein–solvent conformational substates*). Single molecule fluorescence measurements performed in protein–sugar–water systems of different content of residual water (work in progress) evidence different protein families, corresponding to *protein–solvent conformational substates* of different *rigidity levels*, simultaneously present and interconverting. The transition from *hard* to *soft substates* by water uptake appeared to be driven by a cooperative collapse of the HB network anchoring the protein to its surrounding, as suggested by FTIR data (see section 2, figures 5 and 12).

The progressive hindering of the *conformationally gated* QA $\rightarrow$ QB electron transfer in reaction centres from *Rhodobacter Sphaeroides* embedded in trehalose matrices of decreasing residual water [52] was also rationalized on this basis.

4. Conclusions

The reported simulative and experimental data enabled us to infer that the existence of an HB network, which couples the degrees of freedom of the biomolecule to those of the saccharide-containing matrix. In particular, while for a protein the coupling is well described in terms of the *water entrapment* hypothesis, the *water replacement* hypothesis better describes the sugar–membrane interaction; in both cases, the sample water content modulates the strength of the coupling, since the stiffness of the HB network increases by lowering the hydration.

Measurements performed in matrices of different sugars indicated how the protein–matrix coupling, peculiar to each *solvent*, is the tightest in the trehalose systems.

The dependence of the protein–matrix interaction on the detailed *solvent* composition is in line with the lack of 'phase separation' between the protein and the external sugar matrix in trehalose with respect to lactose, found in lysozyme–sugar systems [89]. This effect was suggested to arise from a mismatching between the protein and the sugar–water *structures* at the protein interface [49].

Acknowledgments

This work was supported by MIUR (Grant PRIN 2005, Proprietà Dinamiche Strutturali e Funzionali di Proteine in Sistemi Non-Liquidi Contenenti Acqua Residua: Accoppiamento con la Matrice Esterna) and local fundings (ex 60%).

References

[1] Crowe J H and Crowe L M 1984 *Science* **223** 701–3
[2] Bianchi G, Gamba A, Murellie C, Salamini F and Bartels D 1991 *Plant J.* **1** 355–9
[3] Uritani M, Takai M and Yoshinaga K J 1995 *Biochemistry* **117** 774–9

[4] Panek A D 1995 *J. Med. Biol. Res.* **28** 169–81
[5] Crowe L M 2002 *Comp. Biochem. Physiol.* A **131** 505–13
[6] Crowe J H, Crowe L M and Jackson S A 1983 *Arch. Biochem. Biophys.* **220** 615–7
[7] Crowe L M and Crowe J H 1995 *Liposomes, New Systems and New Trends in their Applications* ed F Puisieux *et al* (Paris: Editions de Santè) pp 237–72
[8] Chiantia S, Giannola L I and Cordone L 2005 *Langmuir* **21** 4108–16
[9] Carpenter J F and Crowe J H 1989 *Biochemistry* **28** 3916–22
[10] Belton P S and Gil A M 1994 *Biopolymers* **34** 957–61
[11] Hagen S J, Hofrichter J and Eaton W A 1995 *Science* **269** 959–62
[12] Hagen S J, Hofrichter J and Eaton W A 1996 *J. Phys. Chem.* **100** 12008–21
[13] Gottfried D S, Peterson E S, Sheikh A G, Wang J, Yang M and Friedman J M 1996 *J. Phys. Chem.* **100** 12034–42
[14] Sastry G M and Agmon N 1997 *Biochemistry* **36** 7097–108
[15] Kleinert T, Doster W, Leyser H, Petry W, Schwarz V and Settles M 1998 *Biochemistry* **37** 717–33
[16] Lichtenegger H, Doster W, Kleinert T, Birk A, Sepiol B and Vogl G 1999 *Biophys. J.* **76** 414–22
[17] Rector D, Jiang J, Berg M A and Fayer M D 2001 *J. Phys. Chem.* B **105** 1081–92
[18] Schlichter J, Friedrich J, Herenyi L and Fidy J 2001 *Biophys. J.* **80** 2011–7
[19] Dantsker D, Samuni U, Friedman A J, Yang M, Ray A and Friedman J M 2002 *J. Mol. Biol.* **315** 239–51
[20] Ponkratov V V, Friedrich J and Vanderkooi J M 2002 *J. Chem. Phys.* **117** 4594–601
[21] Mei E, Tang J, Vanderkooi J M and Hochstrasser J M 2003 *J. Am. Chem. Soc.* **125** 2730–5
[22] Caliskan G, Mechtani D, Roh J H, Kisliuk A, Sokolov A P, Azzam S, Cicerone M T, Lin-Gibson S and Peral I 2004 *J. Chem. Phys.* **121** 1978–83
[23] Massari A M, Finkestein I J, McClain B L, Goj A, Wen X, Bren K L, Loring R F and Fayer M D 2005 *J. Am. Chem. Soc.* **127** 14279–89
[24] Massari A M, Finkelstein I J and Fayer M D 2006 *J. Am. Chem. Soc.* **128** 3990–7
[25] Cordone L, Galajda P, Vitrano E, Gassmann A, Ostermann A and Parak F 1998 *Eur. Biophys. J.* **27** 173–6
[26] Cordone L, Ferrand M, Vitrano E and Zaccai G 1999 *Biophys. J.* **76** 1043–7
[27] Librizzi F, Vitrano E and Cordone L 1999 *Biophys. J.* **76** 2727–34
[28] Librizzi F, Vitrano E and Cordone L 1999 *Biological Physics* ed H Frauenfelder, G Hummer and G G Melville (New York: AIP) pp 132–8
[29] Librizzi F, Paciaroni A, Pfister C, Vitrano E, Zaccai G and Cordone L 2001 *Proc. ILL Millenium Symp. and European User Mtg* (Grenoble: Institute Laue-Langevin) pp 58–9
[30] Cottone G, Cordone L and Ciccotti G 2001 *Biophys. J.* **80** 931–8
[31] Cottone G, Ciccotti G and Cordone L 2002 *J. Chem. Phys.* **117** 9862–6
[32] Lins R D, Pereira C S and Hunenberger P H 2004 *Proteins: Struct. Funct. Bioinformatics* **55** 177–86
[33] Cottone G, Giuffrida S, Ciccotti G and Cordone L 2005 *Proteins: Struct. Funct. Bioinformatics* **59** 291–302
[34] Sum A K, Faller R and de Pablo J J 2003 *Biophys. J.* **85** 2830–44
[35] Pereira C, Lins R D, Chandrasekhar I, Freitas L C G and Hunenberger P H 2004 *Biophys. J.* **86** 2273–85
[36] Villarreal M A, Dyaz S B, Disalvo E A and Montich G G 2004 *Langmuir* **20** 7844–51
[37] Pereira C S and Hunenberger P H 2006 *J. Phys. Chem.* B **110** 15572–81
[38] Allison S D, Chang B, Randolph T W and Carpenter J F 1999 *Arch. Biochem. Biophys.* **365** 289–98
[39] Sampedro J G and Uribe S 2004 *Mol. Cell Biochem.* **256** 319–27
[40] Green J L and Angell C A 1989 *J. Phys. Chem.* **93** 2880–2
[41] Wolkers W F, Oldenhof H, Alberda M and Hoekstra F A 1998 *Biochim. Biophys. Acta* **1379** 83–96
[42] Gaffney S H, Haslam E, Lilley T H and Ward T R 1988 *J. Chem. Soc. Faraday Trans.* **84** 2545–52
[43] Imamura K, Ogawa T, Sakiyama T and Nakanishi K 2003 *J. Pharm. Sci.* **92** 266–74
[44] Magazù S, Maisano G, Migliardo P and Mondelli C 2004 *Biophys. J.* **86** 3241–4
[45] Conrad P B and de Pablo J J 1999 *J. Phys. Chem.* A **103** 4049–55
[46] Ekdawi-Sever N C, Conrad P B and de Pablo J J 2001 *J. Phys. Chem.* A **105** 734–42
[47] Sakurai M, Murata M, Inoue Y, Hino A and Kobayashi S 1997 *Bull. Chem. Soc. Japan* **70** 847–58
[48] Lerbret A, Bordat P, Affouard F, Descamps M and Migliardo F 2005 *J. Phys. Chem.* **109** 11046–57
[49] Giuffrida S, Cottone G and Cordone L 2006 *Biophys. J.* **91** 968–80
[50] Palazzo G, Mallardi A, Hochkoeppler A, Cordone L and Venturoli G 2002 *Biophys. J.* **82** 558–68
[51] Francia F, Palazzo G, Mallardi A, Cordone L and Venturoli G 2003 *Biophys. J.* **85** 2760–75
[52] Francia F, Palazzo G, Mallardi A, Cordone L and Venturoli G 2004 *Biochim. Biophys. Acta—Bioenergetics* **1658** 50–7
[53] Francia F, Giachini L, Palazzo G, Mallardi A, Boscherini F and Venturoli G 2004 *Bioelectrochemistry* **63** 73–7
[54] Librizzi F, Viappiani C, Abbruzzetti S and Cordone L 2002 *J. Chem. Phys.* **116** 1193–200

[55] Giuffrida S, Cottone G, Librizzi F and Cordone L 2003 *J. Phys. Chem.* B **107** 13211–7
[56] Giuffrida S, Cottone G and Cordone L 2004 *J. Phys. Chem.* B **108** 15415–21
[57] Cordone L, Cottone G, Giuffrida S, Palazzo G, Venturoli G and Viappiani C 2005 *Biochim. Biophys. Acta—Proteins Proteomics* **1749** 252–81
[58] Doster W, Bacheitner A, Dunau R, Hiebl M and Luscher E 1986 *Biophys. J.* **50** 213–9
[59] Tarek M and Tobias D J 2000 *Biophys. J.* **79** 3244–57
[60] Tarek M and Tobias D J 2002 *Phys. Rev. Lett.* **88** 8101–4
[61] Frauenfelder H, Parak F and Young R D 1988 *Annu. Rev. Biophys. Chem.* **17** 451–79
[62] Vojtechovsky J, Chu K, Berendzen J, Sweet R M and Schlichting I 1999 *Biophys. J.* **77** 2153–74
[63] Makinen M W, Houtchens R A and Caughey W S 1979 *Proc. Natl Acad. Sci. USA* **76** 6042–6
[64] Beece D, Eisenstein L, Frauenfelder H, Good D, Marden M C, Reinisch L, Reynolds A H, Sorensen L B and Yue K T 1980 *Biochemistry* **19** 5147–57
[65] Doster W, Beece L, Bowne S F, DiIorio E E, Eisenstein L, Frauenfelder H, Reinisch L, Shyamsunder E, Winterhalter K H and Yue K T 1982 *Biochemistry* **21** 4831–9
[66] Frauenfelder H *et al* 1990 *J. Phys. Chem.* **94** 1024–37
[67] Ansari A, Jones C M, Henry E R, Hofrichter J and Eaton W 1992 *Science* **256** 1796–8
[68] Eisenberg D and Kauzmann W 1969 *The Structure and Properties of Water* (London: Oxford University Press)
[69] Kaposi A D, Vanderkooi J M, Wright W W, Fidy J and Stavrov S S 2001 *Biophys. J.* **81** 3472–82
[70] Fenimore P W, Frauenfelder H, McMahon B H and Parak F 2002 *Proc. Natl Acad. Sci. USA* **99** 16047–51
[71] Austin R H, Beeson K W, Eisenstein L, Frauenfelder H and Gunsalus I C 1975 *Biochemistry* **14** 5355–73
[72] Henry E R, Sommer J H, Hofrichter J and Eaton W A 1983 *J. Mol. Biol.* **166** 443–51
[73] Srajer V, Reinisch L and Champion P M 1988 *J. Am. Chem. Soc.* **110** 6656–70
[74] Steinbach P J 1991 *Biochemistry* **30** 3988–4001
[75] Tian W D, Sage J T, Srajer V and Champion P M 1992 *Phys. Rev. Lett.* **68** 408–11
[76] Post F, Doster W, Karvounis G and Settles M 1993 *Biophys. J.* **64** 1833–42
[77] Ansari A, Jones C M, Henry E R, Hofrichter J and Eaton W A 1994 *Biochemistry* **33** 5128–45
[78] McMahon B H, Stojkovic B P, Hay P J, Martin R L and Garcia A E 2000 *J. Chem. Phys.* **113** 6831–50
[79] Chu K, Vojtěchovsky J, McMahon B H, Sweet R M, Berendzen J and Schlichting I 2000 *Nature* **403** 921–3
[80] Ostermann A, Washipky R, Parak F and Nienhaus G U 2000 *Nature* **404** 205–8
[81] Schotte F, Lim M, Jackson T A, Smirnov A V, Soman J, Olson J S Jr, Wulff M and Anfinrud P A 2003 *Science* **300** 1944–7
[82] Abbruzzetti S, Giuffrida S, Sottini S, Viappiani C and Cordone L 2005 *Cell Biochem. Biophys.* **43** 431–8
[83] Boyar H and Severcan F 1997 *J. Mol. Struct.* **408** 269–72
[84] Ceve G and Blume G 2001 *Biochim. Biophys. Acta* **1514** 191–205
[85] Lopez Diez E C and Bone S 2000 *Phys. Med. Biol.* **45** 3577–88
[86] Crowe L 2002 *Comp. Biochem. Physiol.* A **131** 505–13
[87] Ediger M D 2000 *Annu. Rev. Phys. Chem.* **51** 99–128
[88] Roberts C J and Debenedetti P G 1999 *J. Phys. Chem.* B **103** 7308–18
[89] Lam Y H, Bustami R, Phan T, Chan H K and Separovic F 2002 *J. Pharm. Sci.* **91** 943–51